NASA/TM—2008-215424

Air Flow and Pressure Drop Measurements Across Porous Oxides

Dennis S. Fox
Glenn Research Center, Cleveland, Ohio

Michael D. Cuy
ASRC Aerospace Corporation, Cleveland, Ohio

Roger A. Werner (retired)
Glenn Research Center, Cleveland, Ohio

September 2008

NASA STI Program . . . in Profile

Since its founding, NASA has been dedicated to the advancement of aeronautics and space science. The NASA Scientific and Technical Information (STI) program plays a key part in helping NASA maintain this important role.

The NASA STI Program operates under the auspices of the Agency Chief Information Officer. It collects, organizes, provides for archiving, and disseminates NASA's STI. The NASA STI program provides access to the NASA Aeronautics and Space Database and its public interface, the NASA Technical Reports Server, thus providing one of the largest collections of aeronautical and space science STI in the world. Results are published in both non-NASA channels and by NASA in the NASA STI Report Series, which includes the following report types:

- TECHNICAL PUBLICATION. Reports of completed research or a major significant phase of research that present the results of NASA programs and include extensive data or theoretical analysis. Includes compilations of significant scientific and technical data and information deemed to be of continuing reference value. NASA counterpart of peer-reviewed formal professional papers but has less stringent limitations on manuscript length and extent of graphic presentations.

- TECHNICAL MEMORANDUM. Scientific and technical findings that are preliminary or of specialized interest, e.g., quick release reports, working papers, and bibliographies that contain minimal annotation. Does not contain extensive analysis.

- CONTRACTOR REPORT. Scientific and technical findings by NASA-sponsored contractors and grantees.

- CONFERENCE PUBLICATION. Collected papers from scientific and technical conferences, symposia, seminars, or other meetings sponsored or cosponsored by NASA.

- SPECIAL PUBLICATION. Scientific, technical, or historical information from NASA programs, projects, and missions, often concerned with subjects having substantial public interest.

- TECHNICAL TRANSLATION. English-language translations of foreign scientific and technical material pertinent to NASA's mission.

Specialized services also include creating custom thesauri, building customized databases, organizing and publishing research results.

For more information about the NASA STI program, see the following:

- Access the NASA STI program home page at *http://www.sti.nasa.gov*

- E-mail your question via the Internet to *help@sti.nasa.gov*

- Fax your question to the NASA STI Help Desk at 301–621–0134

- Telephone the NASA STI Help Desk at 301–621–0390

- Write to:
  NASA Center for AeroSpace Information (CASI)
  7115 Standard Drive
  Hanover, MD 21076–1320

NASA/TM—2008-215424

Air Flow and Pressure Drop Measurements Across Porous Oxides

Dennis S. Fox
Glenn Research Center, Cleveland, Ohio

Michael D. Cuy
ASRC Aerospace Corporation, Cleveland, Ohio

Roger A. Werner (retired)
Glenn Research Center, Cleveland, Ohio

National Aeronautics and
Space Administration

Glenn Research Center
Cleveland, Ohio 44135

September 2008

Level of Review: This material has been technically reviewed by technical management.

Available from

NASA Center for Aerospace Information
7115 Standard Drive
Hanover, MD 21076–1320

National Technical Information Service
5285 Port Royal Road
Springfield, VA 22161

Available electronically at http://gltrs.grc.nasa.gov

Air Flow and Pressure Drop Measurements Across Porous Oxides

Dennis S. Fox
National Aeronautics and Space Administration
Glenn Research Center
Cleveland, Ohio 44135

Michael D. Cuy
ASRC Aerospace Corporation
Cleveland, Ohio 44135

Roger A. Werner
National Aeronautics and Space Administration
Glenn Research Center
Cleveland, Ohio 44135

Abstract

This report summarizes the results of air flow tests across eight porous, open cell ceramic oxide samples. During ceramic specimen processing, the porosity was formed using the sacrificial template technique, with two different sizes of polystyrene beads used for the template. The samples were initially supplied with thicknesses ranging from 0.14 to 0.20 in. (0.35 to 0.50 cm) and nonuniform backside morphology (some areas dense, some porous). Samples were therefore ground to a thickness of 0.12 to 0.14 in. (0.30 to 0.35 cm) using dry 120 grit SiC paper. Pressure drop versus airflow is reported. Comparisons of samples with thickness variations are made, as are pressure drop estimates. As the density of the ceramic material increases the maximum corrected flow decreases rapidly. Future sample sets should be supplied with samples of similar thickness and having uniform surface morphology. This would allow a more consistent determination of air flow versus processing parameters and the resulting porosity size and distribution.

Introduction

Porous, open cell ceramics are used in a variety of engineering, industrial and aerospace applications. These include hot gas and liquid filters, catalyst and sensor supports, solid oxide fuel cells and chemical reactors (refs. 1 and 2). A comprehensive review of the techniques used to create porous ceramics is found in reference 3. There are three major processing routes (1) replica template, (2) sacrificial template, and (3) direct foaming.

The replica technique uses either a synthetic template or natural cellular template that is infused with a ceramic suspension. Upon drying/firing, the finished ceramic displays the same structure as the template. Templates include naturally occurring sponge, coral, and wood as well as synthetic polymer and carbon foams. In the second technique, a sacrificial phase is homogeneously dispersed within a continuous matrix of ceramic powder particles or a ceramic slip. After processing, pores remain in place of the sacrificial phase. Materials used for the template include polymer beads, salts, and carbon. Natural organic materials for templates include cellulose, sucrose, and wax. Barea et al. (ref. 4) used sacrificial starch to process porous mullite. Finally, liquids such as oils and freeze-dried water or camphene have also been used for templates. Araki and Halloran (ref. 5) used frozen camphene as the template when making porous alumina. The third technique introduces gaseous bubbles into a ceramic suspension. The resulting foam is then stabilized with surfactants to keep the foam structure intact during the firing phase.

Surfactants can be non-ionic, anionic, or cationic. Setting of the foam can be via thermosetting, sol-gel, or gel-casting.

The purpose of the present study is to measure air flow properties of oxide ceramics manufactured using the sacrificial template technique (polymer beads). The desire was to create an open pore structure leading to an air-permeable material. The processing parameters used for the highest-flowing ceramics will be identified. The results will be used by the ceramic manufacturer to guide further processing work.

Procedure

Table I contains initial dimensions and weights of the ceramic specimens. The porosity was formed using the sacrificial template technique. Polystyrene beads were used, with the bead diameter for the PB-1 samples (0.6 to 1 mm) twice that for the PB-2.5 samples (0.36 to 0.5 mm). The rest of the processing specifics remains proprietary to the originator including volume percent of beads used. Photographs of each specimen are contained in appendix A.

The flow apparatus is based on one described in an unpublished report by Sims (ref. 6) The test equipment (figs. 1 and 2) consists of an aluminum "sample assembly", a stainless steel tube (49.5-in. long, 2.350-in. ID, 0.065-in. wall) to insure uniform static pressure at the exit, a clamshell retainer ring, two dial-type 0-35 psig pressure gauges (Pennwalt, Wallace & Tiernan Division), two type-K thermocouples, and a either a 0.32-to-3.2 standard cubic feet per minute (SCFM) or 0.80-to-8.0 SCFM flow meter (Omega FL1501-A or FL4 611-V, respectively). The latter was needed for the three highest flowing specimens: PB2.5-1, PB1-2, and PB2.5-4.

Filtered shop air is routed through the flow meter to the sample assembly. The assembly (figs. 3, 4, and 5) contains a flow orifice, the ceramic sample, a rubber gasket and a downstream flow orifice. Three flow orifices are available to use: 0.07-in., 0.125-in. or 0.250-in. inside diameter. If the samples are somewhat restrictive to air flow, only the largest orifice provides useful data—as was the case in this study.

The inside diameter of the downstream flow orifice is 1.747 in., providing an exit area of 2.397 $in.^2$. The outer diameters of the flow orifices are sealed in the sample assembly with O-rings. Initial calibration of each flow orifice was conducted with no ceramic sample in place. The results are displayed in figure 6. Inlet pressure and temperature are measured upstream of the sample as shown in figure 3; the exit pressure and temperature is measured at the far end of the steel tube. The flow is so low at these measurement locations that total and static pressure are identical.

In preparation for the test each sample is "potted" into an aluminum ring using room-temperature vulcanizing rubber (RTV). Figure 7 is a representative cross section of such a ring. The thicknesses of the available aluminum rings range from 0.11 to 0.13 in. Because of this and the fact that the backside morphology of the as-received samples showed various levels of porosity—or lack thereof (see Results section and appendix A), the backside of each sample was ground (dry) using 120 grit SiC paper. The resulting thicknesses are listed in table II.

Once each sample was loaded into the flow apparatus, the upstream sample pressure was increased in 1 psi increments up to a maximum of 15 psi over ambient by adjusting the flow meter control knob. Airflow in SCFM was manually logged in a laboratory notebook. Upstream sample inlet temperature, downstream outlet temperature, and outlet pressure were logged at test start; these numbers did not vary throughout the flow test. The contribution of pressure loss by the orifice to the sample ΔP is negligible.

Because all samples exhibited good flow throughout the 15 Δpsi pressure range, a *corrected* ΔP was calculated by taking into account the ambient air pressure and measured sample inlet temperature. The procedure (ref. 6) is as follows, where

corrected $\Delta P = \sigma$ x measured ΔP
$\sigma = \rho_{test}/\rho_{stp}$, and

$\rho_{stp} = 0.0765$ lb/ft^3
$\rho_{test} = \dfrac{(\text{Ambient atmospheric pressure} + \text{measured } \Delta P) \times 144}{(\text{Inlet temperature} + 459.67) \times 53.352}$

Atmospheric pressure and ΔP are measured in psi and inlet temperature is measured in °F. SCFM versus corrected ΔP was input into a spreadsheet and graphed (appendix B).

Results and Discussion

The top two photographs in each appendix A figure are of the as-received material, with the side having the identification number designated with the front side. Note that in most cases the as-received backside had an inconsistent morphology with some areas exhibiting porosity and other areas seemingly very dense. The backside surfaces in general were also not flat. For this reason, the backside of each sample was ground (dry) using 120 grit SiC paper. The resulting thicknesses are listed in table II.

Appendix B contains the air flow data for each material. None of the specimens flowed well with the 0.125-in. flow orifice installed. Air did flow through all samples using the 0.250-in. flow orifice up to 15 delta psi. Specimens PB1-2 and PB1-3 became cracked (the latter more than the former) at some point during the flow testing. These cracks were not catastrophic, but likely allowed somewhat more air to pass during the testing. Note the anomaly in flow for sample PB1-3 in figures 8 and 9. The crack appears to have occurred as the corrected ΔP was raised from 42 to 54 psid (ΔP from 4 to 5 psid).

Figure 8 compares the sample results individually presented in appendix B. Figure 9 uses the data but normalizes the ΔP with the inlet pressure and divides by the sample thickness. This allows for comparisons of samples with thickness variations and provides some data for pressure drop estimates as the thickness is changed. Since the inlet pressure increases with ΔP for a sample test, both SCFM and mass flow will also increase. The characterization of sample ΔP with flow can better be determined if corrected mass flow were used.

$$\text{Corrected mass flow} = \frac{(\text{mass flow}) \times \text{sqrt}(\text{Inlet temperature °F} + 459.67)}{(\text{Inlet pressure}/\text{Pstd}) \times \text{sqrt}(\text{Tstd})}$$

where Pstd = 14.696 psia and Tstd = 518.67 R.

The corrected mass flow is also divided by the flow area of the 0.250-in. orifice (0.04909 in.^{2}). Figure 9 shows that the mass flow of the samples becomes constant or choked as the ΔP increases.

Figure 10 presents the pressure drop data for constant levels of corrected airflow as a function of the sample density. Figure 11 takes estimates of the maximum or choked corrected airflow from figure 9 and are plotted against sample density. As the density of the ceramic material increases, the maximum corrected flow decreases rapidly.

The ranking of the specimens in order from those allowing the highest flow rate at 15 psi ΔP to the lowest is listed in table III. Also listed are the initial and final sample thicknesses, as well as the change in thickness due to grinding. Note that the sample that exhibited the most cracking (PB1-3) was the second lowest flowing specimen. The pressure build-up causes such cracks to form.

Conclusion

The PB2.5 processing route results in more-porous specimens that flow greater amounts of air than those processed via PB1. It should be noted that any future sample set should be supplied with each specimen in the batch having the same thickness. A uniform backside morphology with a consistent porosity is also highly desired. Eliminating these variables would allow a more consistent determination

of air flow versus processing parameters/porosity size/distribution. The nonuniformity of the sample density/surface, combined with the small flow orifice, likely caused variations in the reported data. More consistent results could be achieved with a larger orifice.

TABLE I.—INITIAL (THICK) SAMPLE WEIGHT/DIMENSION/DENSITY

	Wgt, g	Wgt, lb	Thickness, in.	Dia., in.	Vol., $in.^3$	Density, $lb/in.^3$	Thickness, cm	Dia., cm	Vol., cc	Density, g/cc
PB1-1	10.49	0.023	0.200	1.98	0.62	0.038	0.508	5.03	10.1	1.04
PB1-2	10.41	0.023	0.197	1.99	0.61	0.037	0.500	5.05	10.0	1.04
PB1-3	8.30	0.018	0.146	1.98	0.45	0.041	0.371	5.03	7.4	1.13
PB1-4	8.87	0.020	0.152	1.98	0.47	0.042	0.386	5.03	7.7	1.16
PB2.5-1	10.18	0.022	0.200	1.98	0.62	0.036	0.508	5.03	10.1	1.01
PB2.5-2	10.59	0.023	0.190	1.98	0.58	0.040	0.483	5.03	9.6	1.10
PB2.5-3	7.83	0.017	0.138	1.98	0.42	0.041	0.351	5.03	7.0	1.12
PB2.5-4	8.03	0.018	0.153	1.98	0.47	0.038	0.389	5.03	7.7	1.04

TABLE II.—AS-TESTED (GROUND THICKNESS) SAMPLE WEIGHT/DIMENSION/DENSITY

	Wgt, g	Wgt, lb	Thickness, in.	Dia., in.	Vol., $in.^3$	Density, $lb/in.^3$	Thickness, cm	Dia., cm	Vol., cc	Density, g/cc
PB1-1	7.22	0.016	0.132	1.98	0.41	0.039	0.335	5.03	6.7	1.08
PB1-2	6.62	0.015	0.129	1.99	0.40	0.036	0.328	5.05	6.6	1.01
PB1-3	7.12	0.016	0.121	1.98	0.37	0.042	0.307	5.03	6.1	1.17
PB1-4	7.94	0.018	0.135	1.98	0.42	0.042	0.343	5.03	6.8	1.17
PB2.5-1	6.66	0.015	0.133	1.98	0.41	0.036	0.338	5.03	6.7	0.99
PB2.5-2	7.56	0.017	0.135	1.98	0.42	0.040	0.343	5.03	6.8	1.11
PB2.5-3	6.29	0.014	0.116	1.98	0.36	0.039	0.295	5.03	5.9	1.07
PB2.5-4	6.06	0.013	0.116	1.98	0.36	0.037	0.295	5.03	5.9	1.04

TABLE III.—RANKING OF HIGHEST FLOW AT Δ15 psi

	Flow		Initial thickness		As-ground thickness		Delta thickness	
	SCFM	lb/min	in.	cm	in.	cm	in.	cm
PB2.5-1	4.40	0.330	0.200	0.508	0.133	0.338	0.07	0.17
PB1-2	3.90	0.293	0.197	0.500	0.129	0.328	0.07	0.17
PB2.5-4	3.70	0.278	0.153	0.389	0.116	0.295	0.04	0.09
PB2.5-3	2.73	0.205	0.138	0.351	0.116	0.295	0.02	0.06
PB1-1	2.69	0.202	0.200	0.508	0.132	0.335	0.07	0.17
PB2.5-2	2.66	0.200	0.190	0.483	0.135	0.343	0.06	0.14
PB1-3	1.86	0.140	0.146	0.371	0.121	0.307	0.03	0.06
PB1-4	0.92	0.069	0.152	0.386	0.135	0.343	0.02	0.04

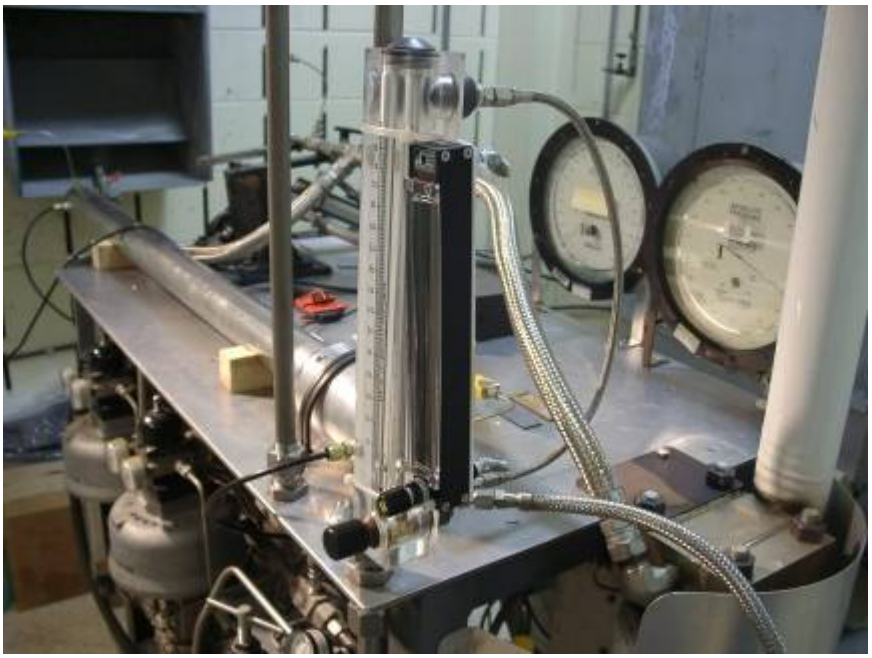

Figure 1.—Complete flow apparatus.

Figure 2.—Pressure gauges and flowmeter.

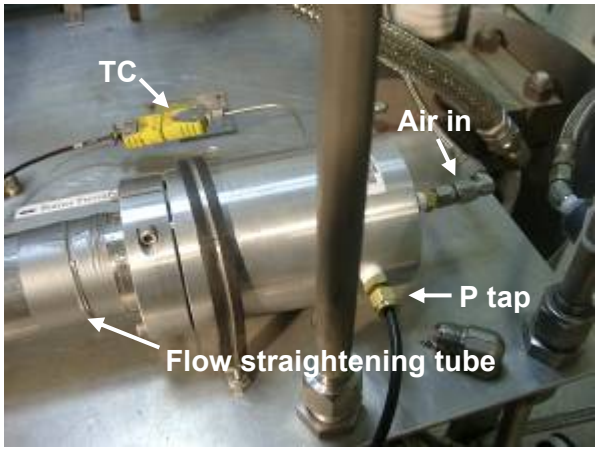

Figure 3.—Sample assembly in place.

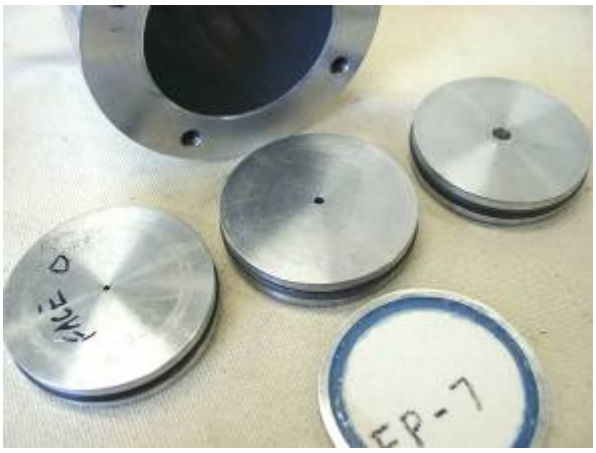

Figure 4.—Flow orifices: 0.07, 0.125, 0.250 in. (L to R). All disc ODs = 2.495 in.

Figure 5.—Sample insertion order: flow orifice, potted sample (RTV faces upstream), gasket, downstream orifice.

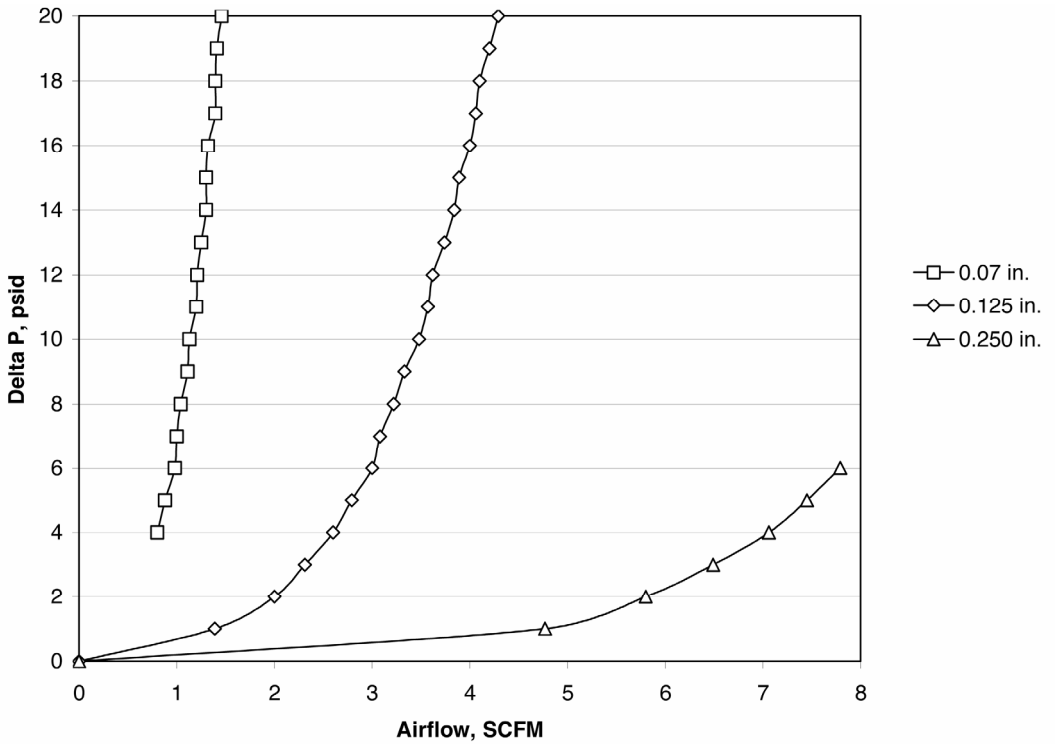

Figure 6.—Air flow rate (SCFM) versus delta pressure (psid) for each flow orifice alone (no sample loaded).

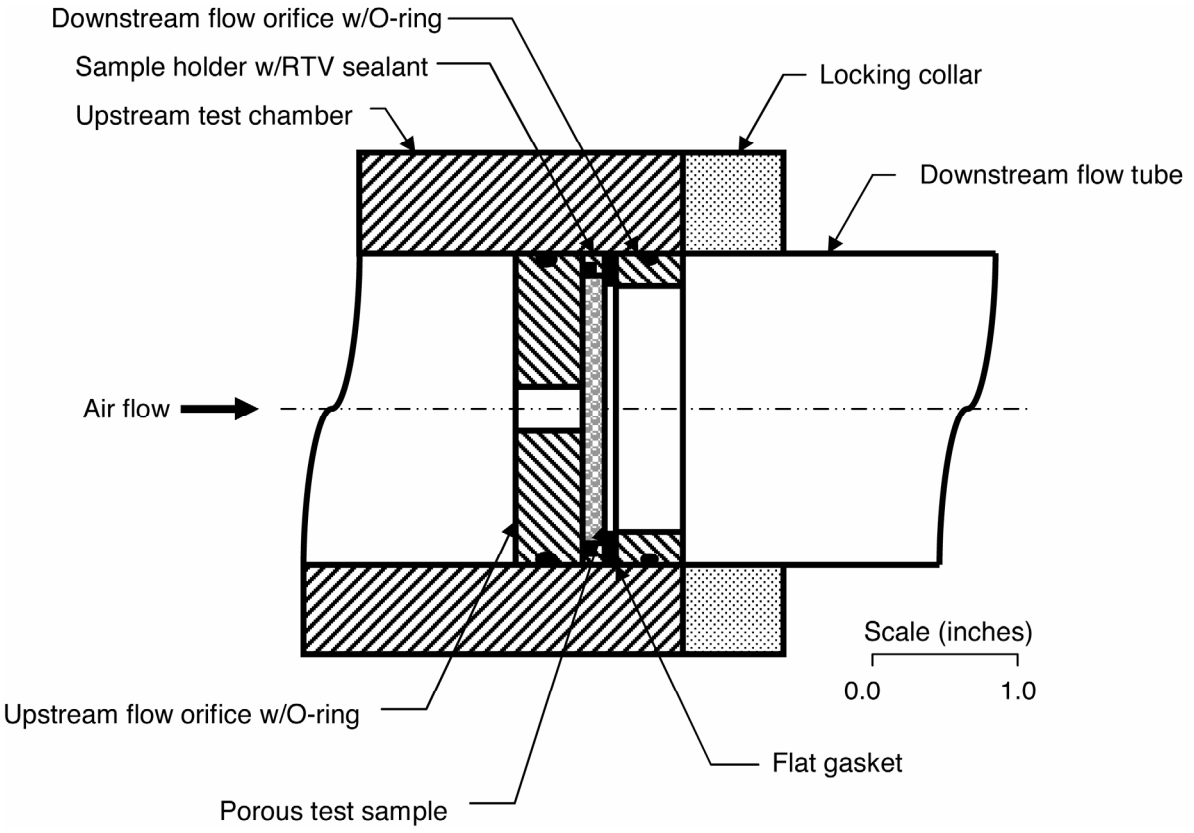

Figure 7.—Test set-up cross-section.

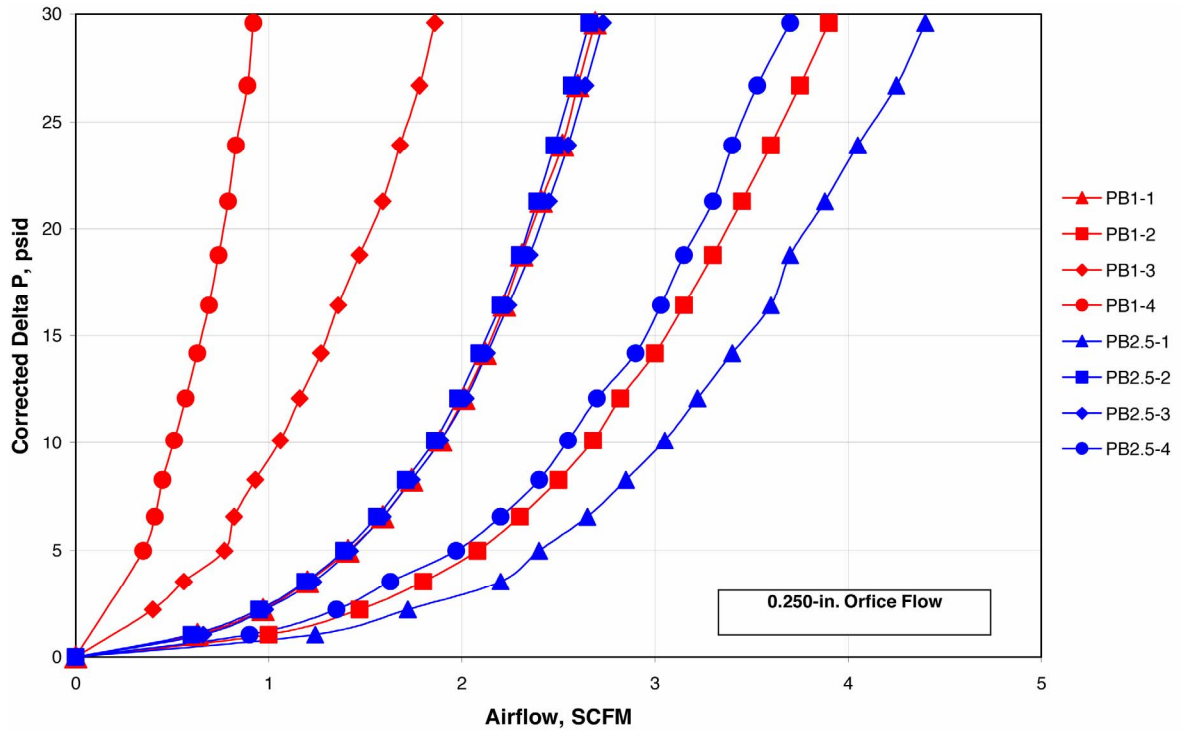

Figure 8.—Sample comparisons, pressure drop versus airflow.

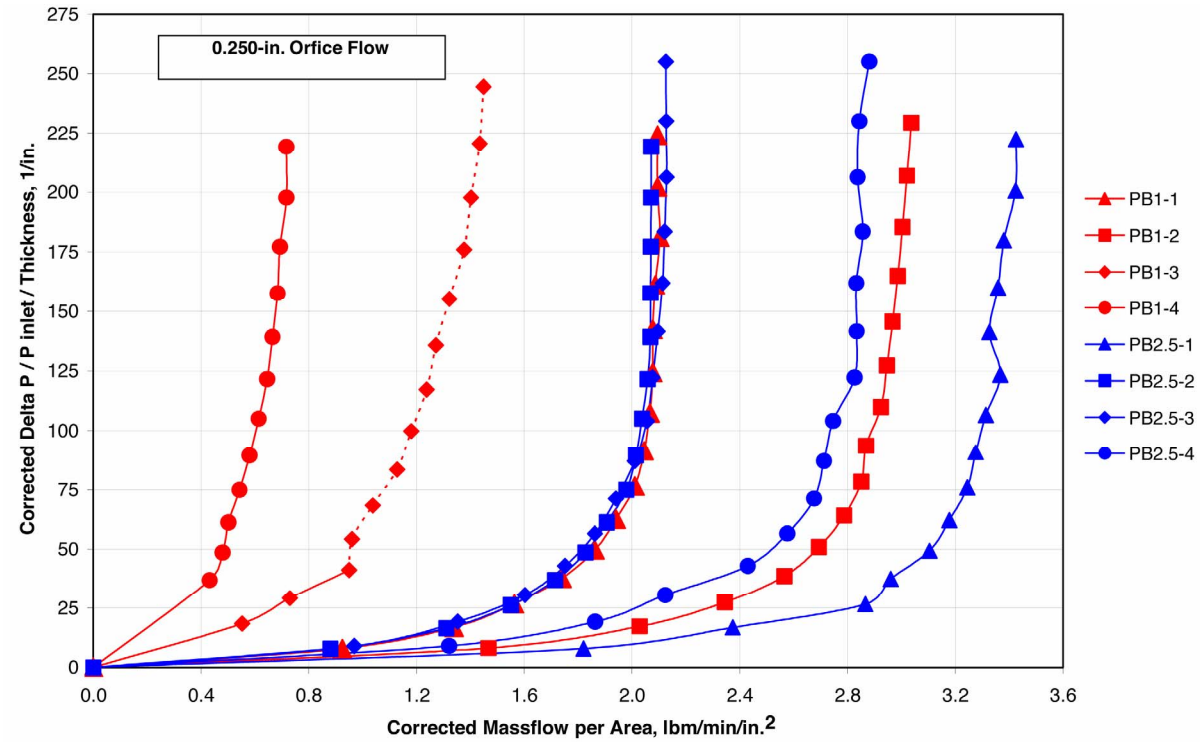

Figure 9.—Sample corrected pressure drop over inlet pressure per sample thickness versus corrected mass flow per orifice flow area.

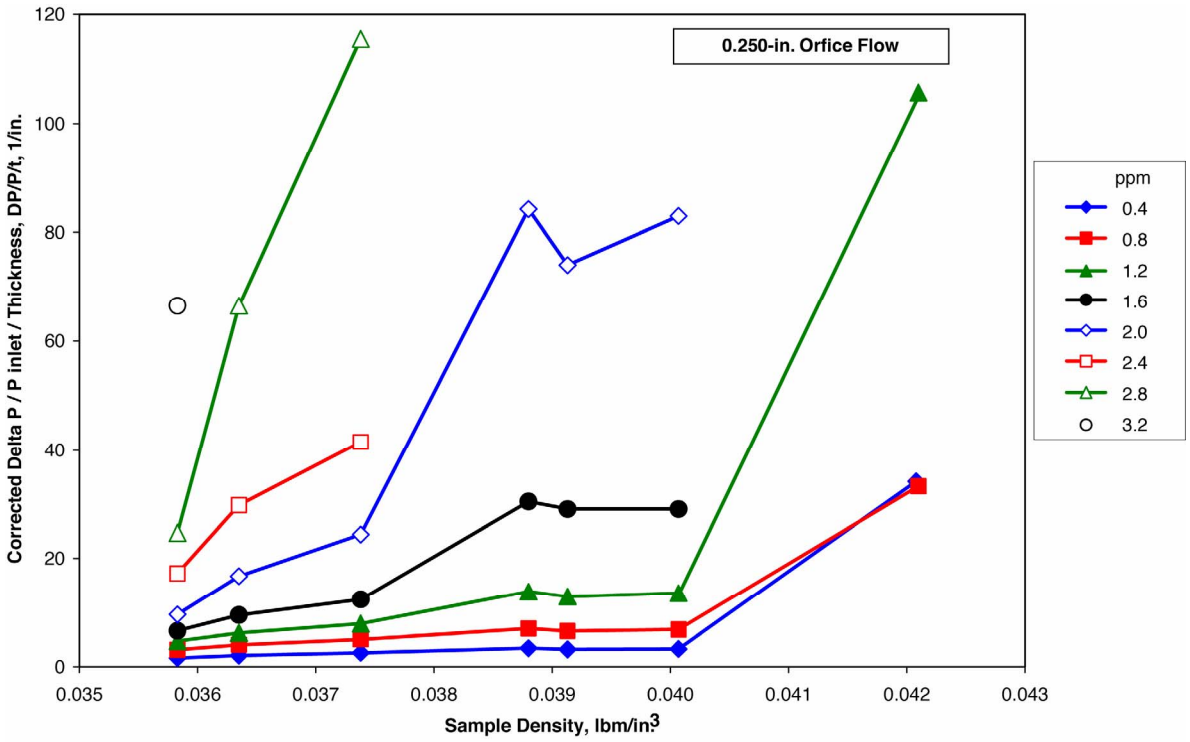

Figure 10.—Cross-plot of figure 9 showing corrected pressure drop per inch at constant corrected mass flows per area versus sample density.

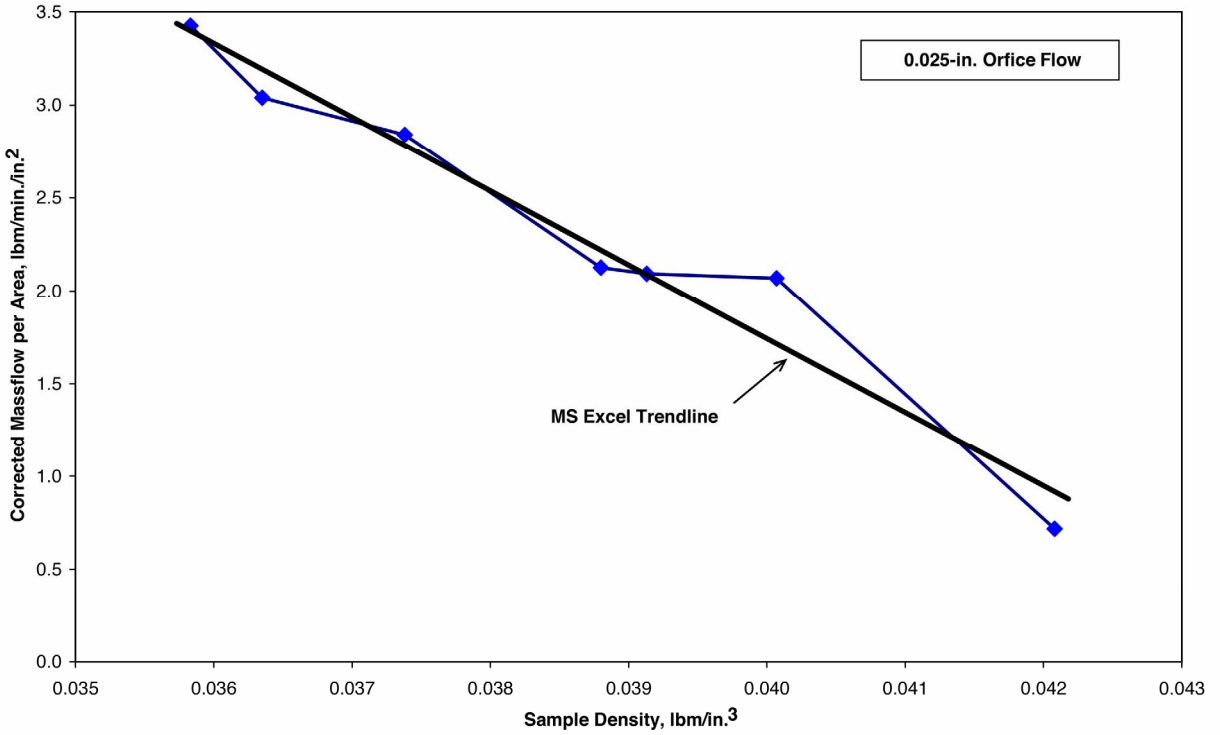

Figure 11.—Estimated choked corrected mass flow per unit area from figure 9 versus sample density.

Appendix A

Macrographs

(1) Front side (with ID);
(2) Backside as-received;
(3) Backside ground

PB1-1
PB1-2
PB1-3
PB1-4

PB2.5-1
PB2.5-2
PB2.5-3
PB2.5-4

Figure 12.—Sample PB1-1 (front and back as-received; back as-sanded).

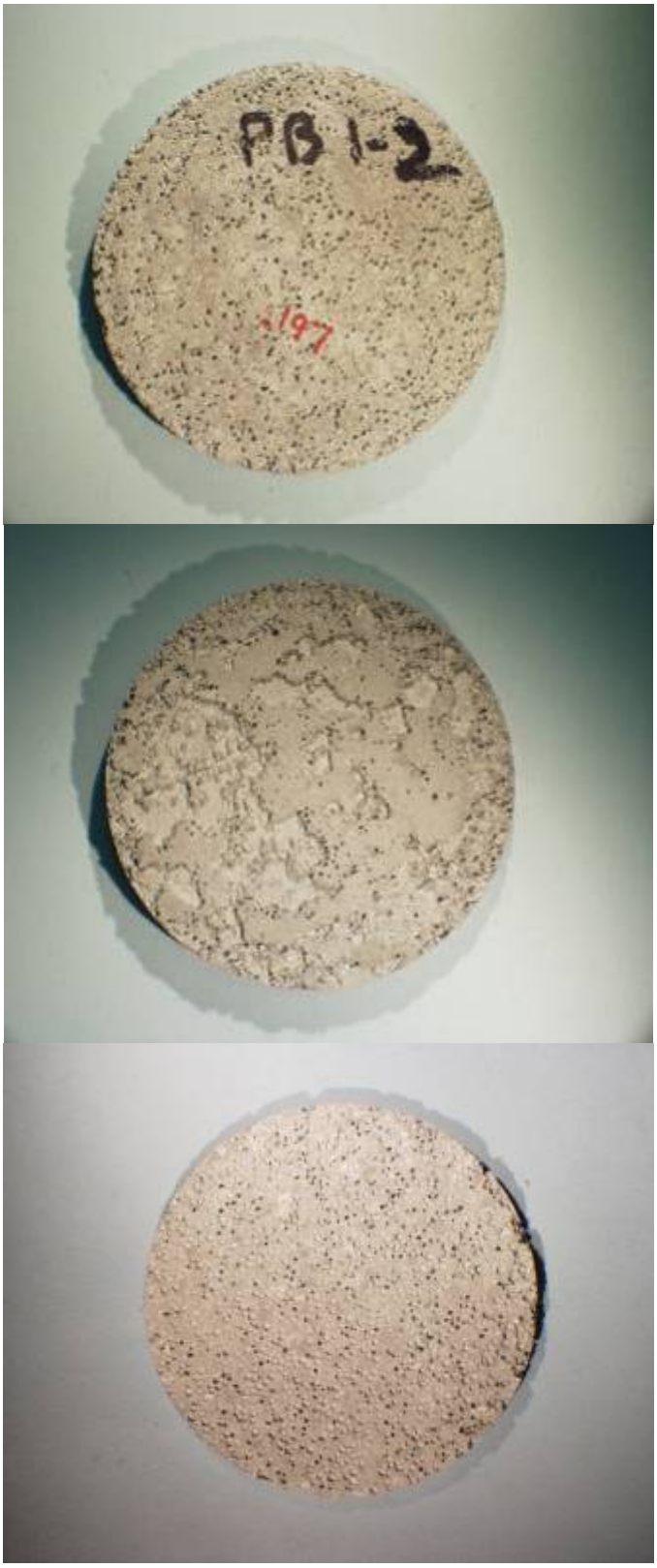

Figure 13.—Sample PB1-2 (front and back as-received; back as-sanded).

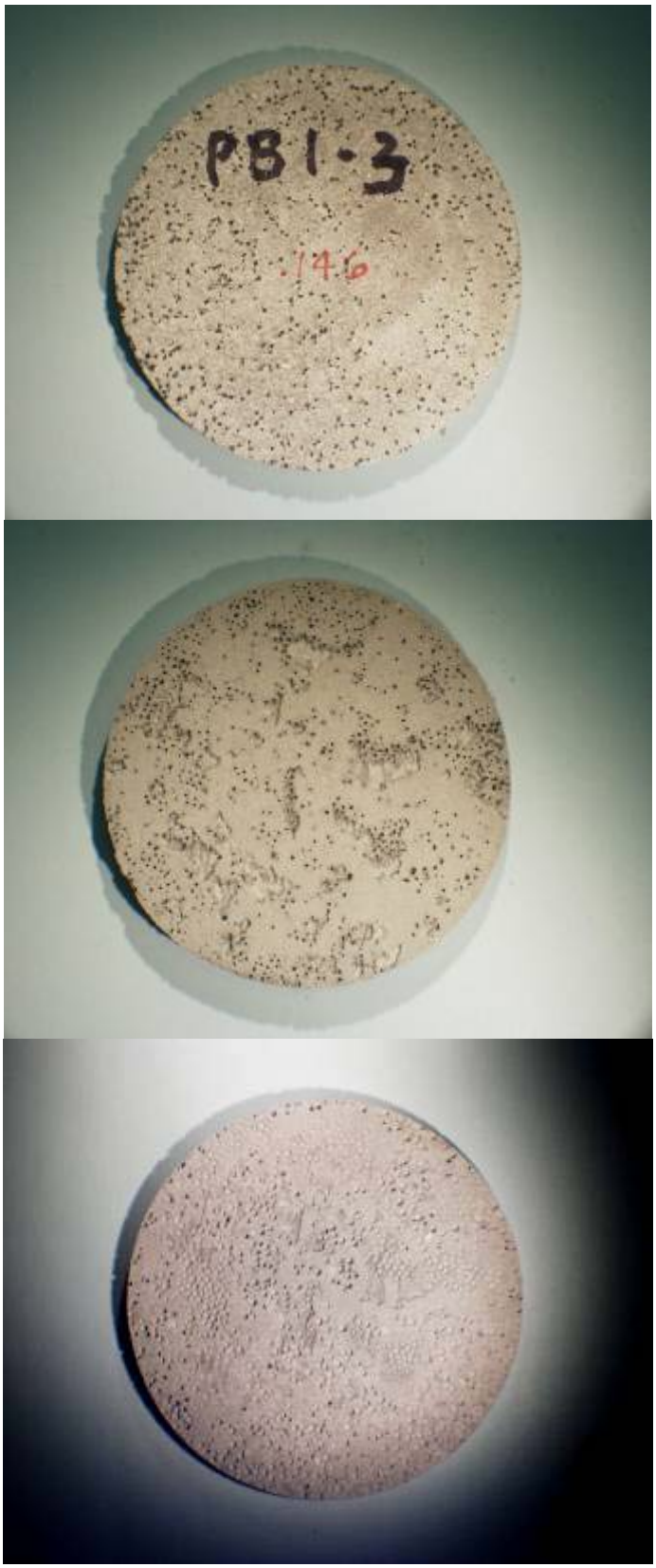

Figure 14.—Sample PB1-3 (front and back as-received; back as-sanded).

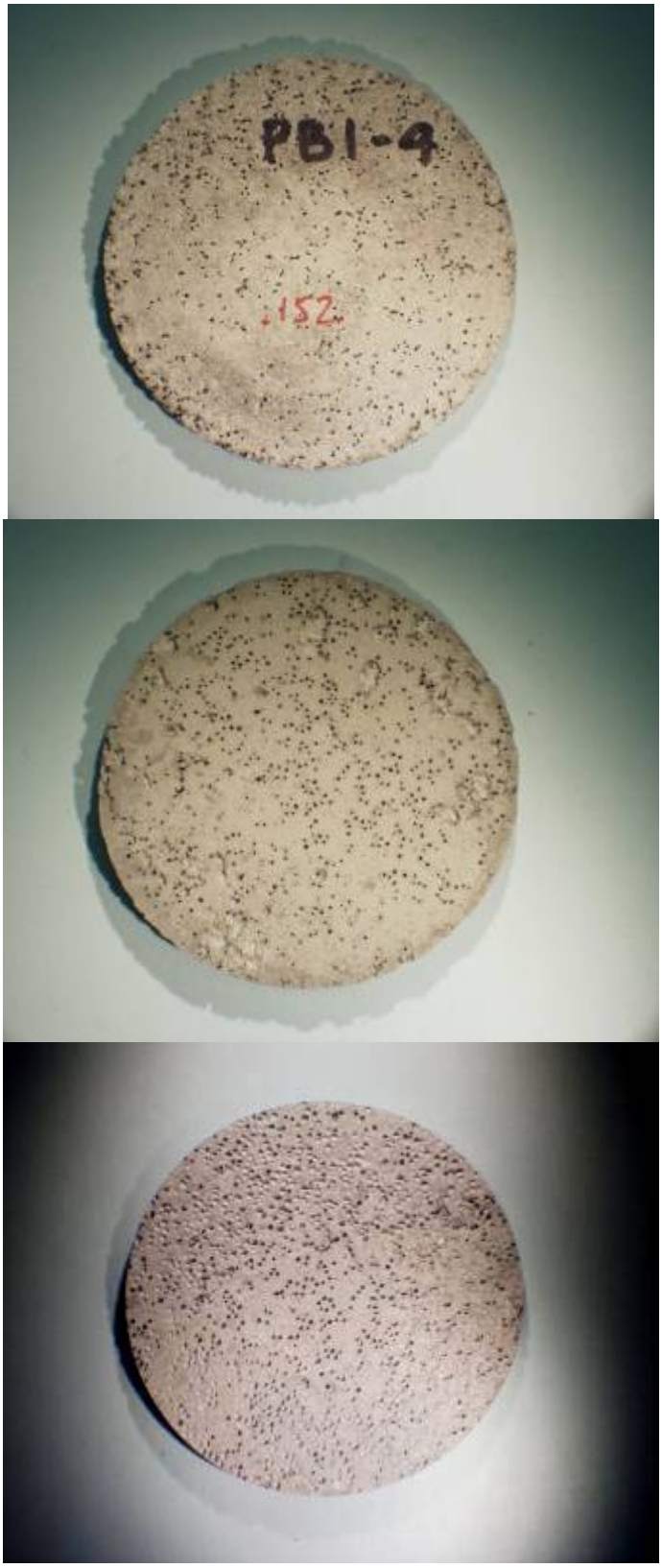

Figure 15.—Sample PB1-4 (front and back as-received; back as-sanded).

Figure 16.—Sample PB2.5-1 (front and back as-received; back as-sanded).

Figure 17.—Sample PB2.5-2 (front and back as-received; back as-sanded).

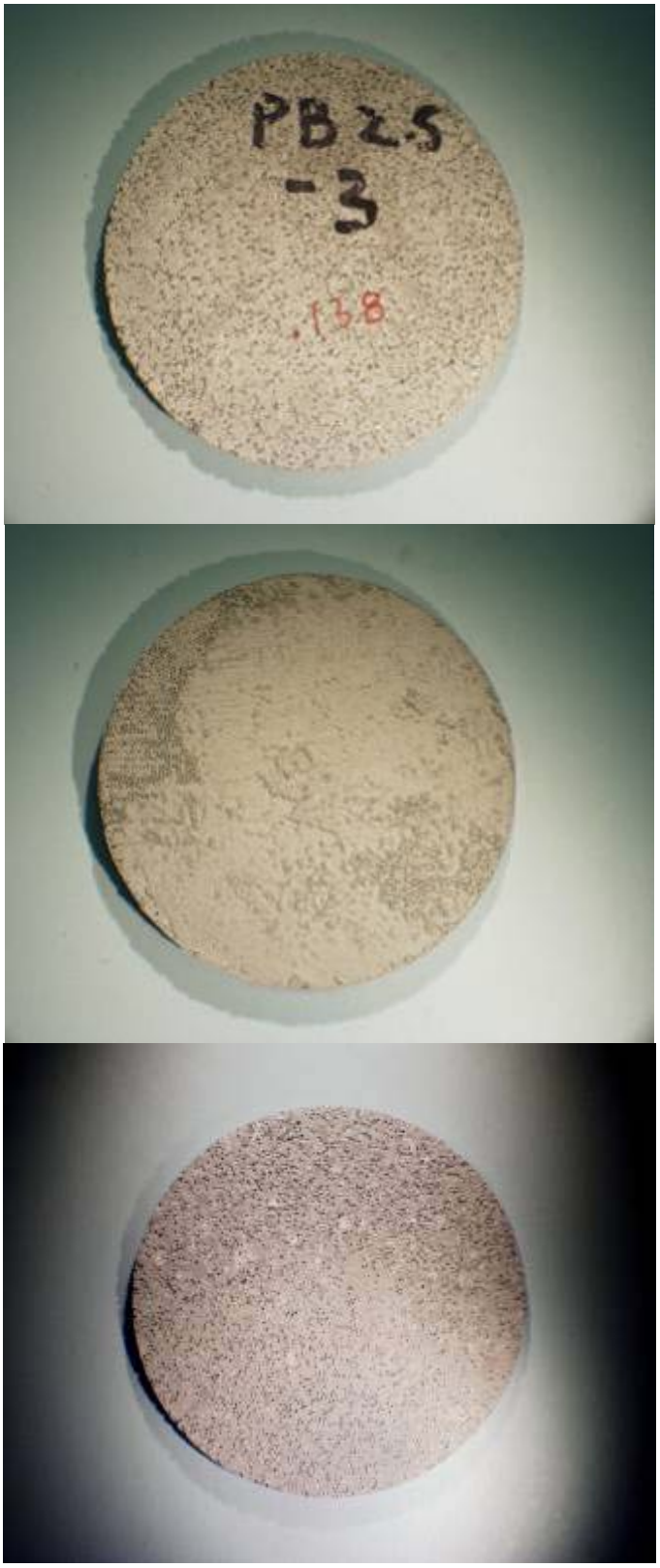

Figure 18.—Sample PB2.5-3 (front and back as-received; back as-sanded).

Figure 19.—Sample PB2.5-4 (front and back as-received; back as-sanded).

Appendix B

SCFM versus corrected ΔP

PB1-1
PB1-2
PB1-3
PB1-4

PB2.5-1
PB2.5-2
PB2.5-3
PB2.5-4

Δpsi		Flow, SCFM	
Meas	Corr	0.250 in.	Data
0	0.00	0.00	0.00
1	1.05	4.77	0.63
2	2.23	5.80	0.97
3	3.54	6.49	1.20
4	4.98	7.06	1.41
5	6.56	7.46	1.59
6	8.27	7.79	1.74
7	10.11		1.89
8	12.08		2.01
9	14.18		2.12
10	16.42		2.22
11	18.79		2.31
12	21.29		2.41
13	23.93		2.52
14	26.69		2.60
15	29.59		2.69

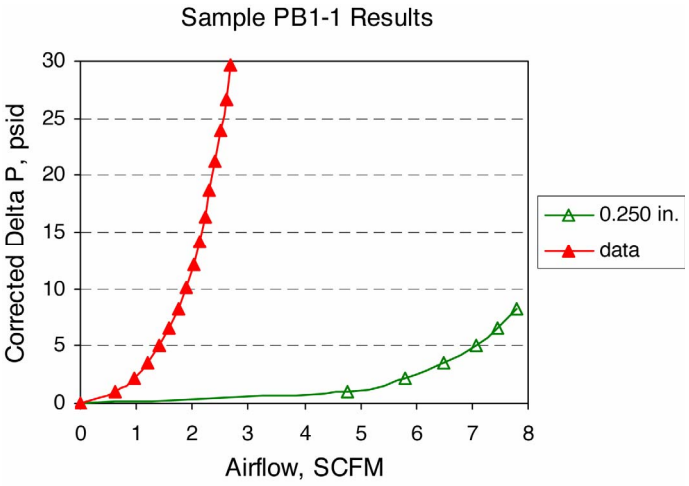

Δpsi		Flow, SCFM	
Meas	Corr	0.250 in.	Data
0	0.00	0.00	0.00
1	1.05	4.77	1.00
2	2.23	5.80	1.47
3	3.54	6.49	1.80
4	4.98	7.06	2.08
5	6.56	7.46	2.30
6	8.27	7.79	2.50
7	10.11		2.68
8	12.08		2.82
9	14.18		3.00
10	16.42		3.15
11	18.79		3.30
12	21.29		3.45
13	23.93		3.60
14	26.69		3.75
15	29.59		3.90

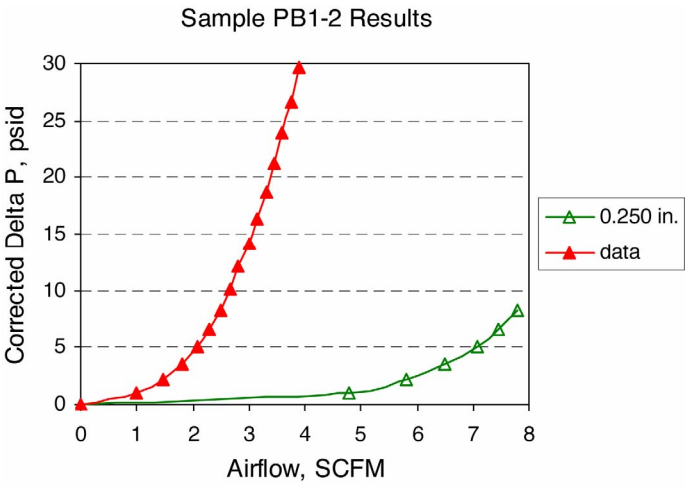

Δpsi		Flow, SCFM	
Meas	Corr	0.250 in.	Data
0	0.00	0.00	0.00
1	1.05	4.77	
2	2.23	5.80	0.40
3	3.54	6.49	0.56
4	4.98	7.06	0.77
5	6.56	7.46	0.82
6	8.27	7.79	0.93
7	10.11		1.06
8	12.08		1.16
9	14.18		1.27
10	16.42		1.36
11	18.79		1.47
12	21.29		1.59
13	23.93		1.68
14	26.69		1.78
15	29.59		1.86

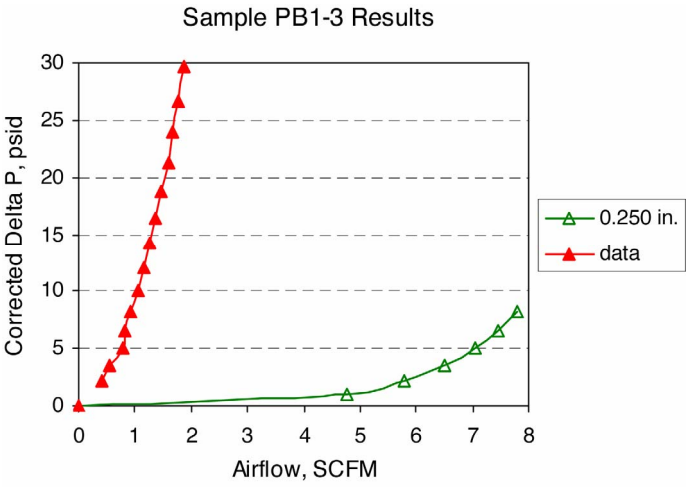

Δpsi		Flow, SCFM	
Meas	Corr	0.250 in.	Data
0	0.00	0.00	0.00
1	1.05	4.77	
2	2.23	5.80	
3	3.54	6.49	
4	4.98	7.06	0.35
5	6.56	7.46	0.41
6	8.27	7.79	0.45
7	10.11		0.51
8	12.08		0.57
9	14.18		0.63
10	16.42		0.69
11	18.79		0.74
12	21.29		0.79
13	23.93		0.83
14	26.69		0.89
15	29.59		0.92

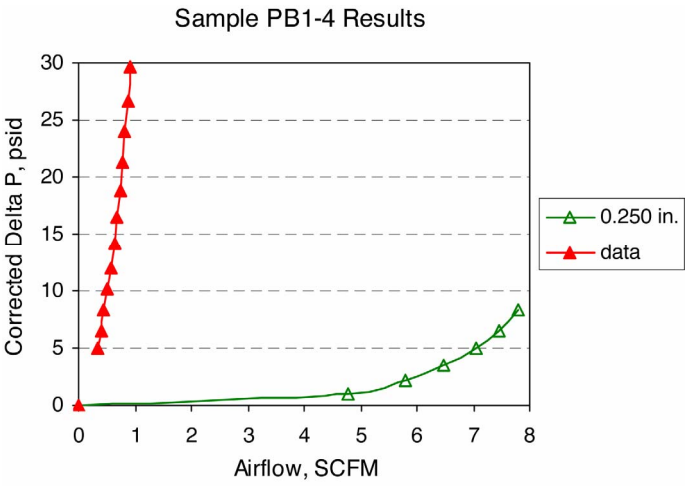

Δpsi		Flow, SCFM	
Meas	Corr	0.250 in.	Data
0	0.00	0.00	0.00
1	1.05	4.77	1.24
2	2.23	5.80	1.72
3	3.54	6.49	2.20
4	4.98	7.06	2.40
5	6.56	7.46	2.65
6	8.27	7.79	2.85
7	10.11		3.05
8	12.08		3.22
9	14.18		3.40
10	16.42		3.60
11	18.79		3.70
12	21.29		3.88
13	23.93		4.05
14	26.69		4.25
15	29.59		4.40

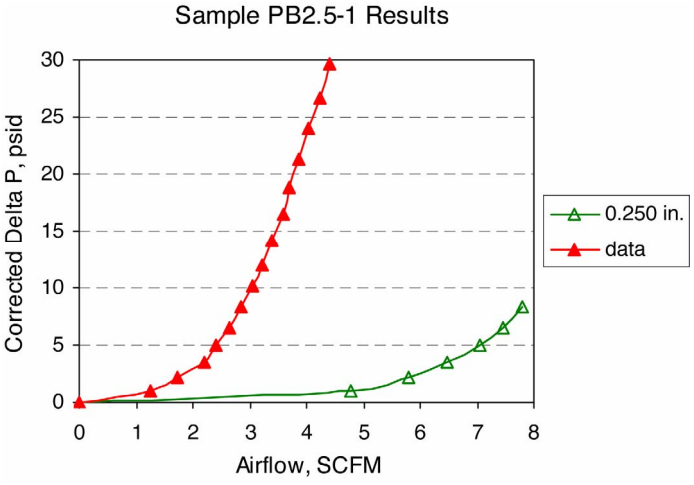

Δpsi		Flow, SCFM	
Meas	Corr	0.250 in.	Data
0	0.00	0.00	0.00
1	1.05	4.77	0.60
2	2.23	5.80	0.95
3	3.54	6.49	1.19
4	4.98	7.06	1.39
5	6.56	7.46	1.56
6	8.27	7.79	1.71
7	10.11		1.86
8	12.08		1.98
9	14.18		2.09
10	16.42		2.20
11	18.79		2.30
12	21.29		2.39
13	23.93		2.48
14	26.69		2.57
15	29.59		2.66

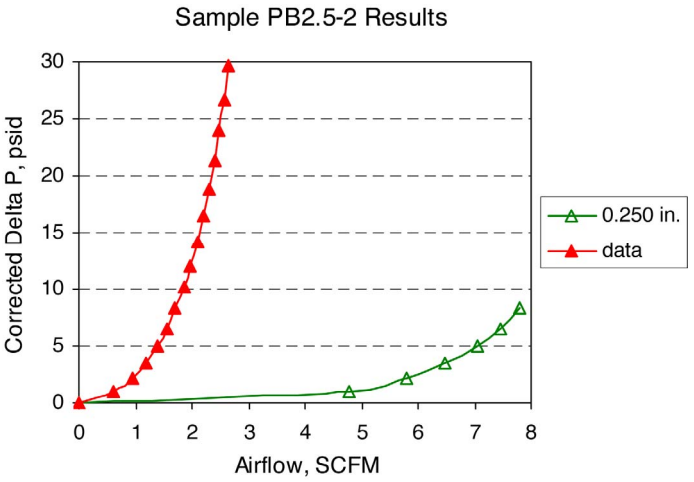

Δpsi		Flow, SCFM	
Meas	Corr	0.250 in.	Data
0	0.00	0.00	0.00
1	1.05	4.77	0.66
2	2.23	5.80	0.98
3	3.54	6.49	1.23
4	4.98	7.06	1.42
5	6.56	7.46	1.59
6	8.27	7.79	1.74
7	10.11		1.89
8	12.08		2.02
9	14.18		2.13
10	16.42		2.24
11	18.79		2.35
12	21.29		2.45
13	23.93		2.55
14	26.69		2.64
15	29.59		2.73

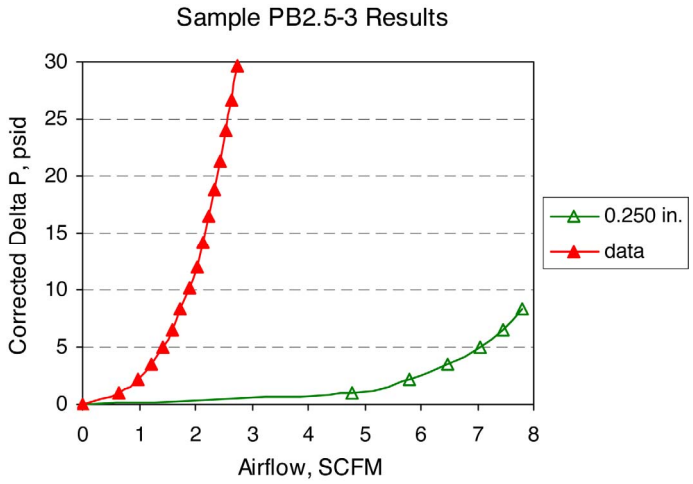

Δpsi		Flow, SCFM	
Meas	Corr	0.250 in.	Data
0	0.00	0.00	0.00
1	1.05	4.77	0.90
2	2.23	5.80	1.35
3	3.54	6.49	1.63
4	4.98	7.06	1.97
5	6.56	7.46	2.20
6	8.27	7.79	2.40
7	10.11		2.55
8	12.08		2.70
9	14.18		2.90
10	16.42		3.03
11	18.79		3.15
12	21.29		3.30
13	23.93		3.40
14	26.69		3.53
15	29.59		3.70

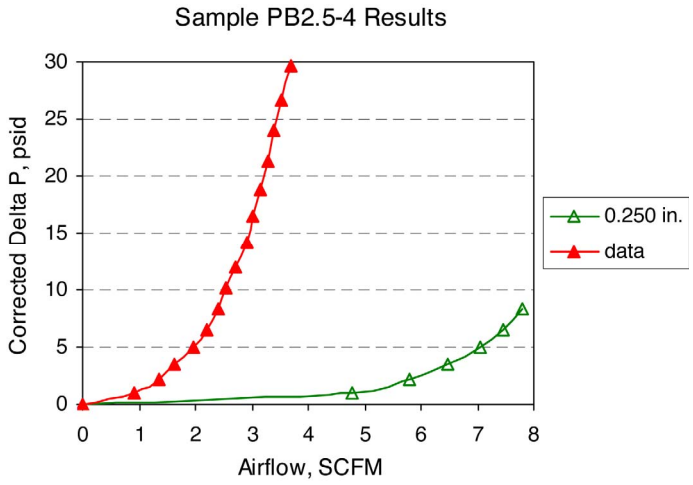

References

1. Green, D.J. and Colombo, P., "Cellular Ceramics: Intriguing Structures, Novel Properties, and Innovative Applications," MRS Bull., 28 [4] (2003) 296–300.
2. Cellular Ceramics: Structure, Manufacturing, Properties and Applications, M. Scheffler and P. Colombo, eds., Wiley-VCH, 2005.
3. Studart, A.R.; Gonzenbach, U.T.; Tervoort, E.; and Gauckler, L.J.: "Processing Routes to Macroporous Ceramics: A Review," *J. Am. Ceram. Soc.,* vol. 89, no. 6, 2006, pp. 1771–1789.
4. Barea, R., Osendi, M.I., Miranzow, P., and Ferreira, J.M.F.: "Fabrication of Highly Porous Mullite Materials," *J. Am. Ceram. Soc.,* vol. 88 no. 3, 2005, pp. 777–779.
5. Araki, K. and Halloran, J.W.: "Porous Ceramic Bodies With Interconnected Pore Channels by a Novel Freeze Casting Technique, "*J. Am. Ceram. Soc*., vol. 88 no. 5, 2005, pp. 1108–1114.
6. Sims, J.R.: "Air Flow Properties Testing of Porous Media," unpublished internal report, The Boeing Company (March 1998).

REPORT DOCUMENTATION PAGE			Form Approved OMB No. 0704-0188

1. REPORT DATE *(DD-MM-YYYY)*	2. REPORT TYPE	3. DATES COVERED *(From - To)*
01-09-2008	Technical Memorandum	

4. TITLE AND SUBTITLE
Air Flow and Pressure Drop Measurements

5a. CONTRACT NUMBER

5b. GRANT NUMBER

5c. PROGRAM ELEMENT NUMBER

6. AUTHOR(S)
Fox, Dennis, S.; Cuy, Michael, D.; Werner, Roger, A.

5d. PROJECT NUMBER

5e. TASK NUMBER

5f. WORK UNIT NUMBER
WBS 561581.02.10.03.03

7. PERFORMING ORGANIZATION NAME(S) AND ADDRESS(ES)
National Aeronautics and Space Administration
John H. Glenn Research Center at Lewis Field
Cleveland, Ohio 44135-3191

8. PERFORMING ORGANIZATION REPORT NUMBER
E-16596

9. SPONSORING/MONITORING AGENCY NAME(S) AND ADDRESS(ES)
National Aeronautics and Space Administration
Washington, DC 20546-0001

10. SPONSORING/MONITORS ACRONYM(S)
NASA

11. SPONSORING/MONITORING REPORT NUMBER
NASA/TM-2008-215424

12. DISTRIBUTION/AVAILABILITY STATEMENT
Unclassified-Unlimited
Subject Categories: 27 and 34
Available electronically at http://gltrs.grc.nasa.gov
This publication is available from the NASA Center for AeroSpace Information, 301-621-0390

13. SUPPLEMENTARY NOTES
Rodger A. Werner (retired), NASA Glenn Research Center. Responsible person, Dennis S. Fox, organization code RXD0, 216-433-3295.

14. ABSTRACT
This report summarizes the results of air flow tests across eight porous, open cell ceramic oxide samples. During ceramic specimen processing, the porosity was formed using the sacrificial template technique, with two different sizes of polystyrene beads used for the template. The samples were initially supplied with thicknesses ranging from 0.14 to 0.20 in. (0.35 to 0.50 cm) and nonuniform backside morphology (some areas dense, some porous). Samples were therefore ground to a thickness of 0.12 to 0.14 in. (0.30 to 0.35 cm) using dry 120 grit SiC paper. Pressure drop versus air flow is reported. Comparisons of samples with thickness variations are made, as are pressure drop estimates. As the density of the ceramic material increases the maximum corrected flow decreases rapidly. Future sample sets should be supplied with samples of similar thickness and having uniform surface morphology. This would allow a more consistent determination of air flow versus processing parameters and the resulting porosity size and distribution.

15. SUBJECT TERMS
Ceramics; Porosity; Air flow

16. SECURITY CLASSIFICATION OF:			17. LIMITATION OF ABSTRACT	18. NUMBER OF PAGES	19a. NAME OF RESPONSIBLE PERSON
a. REPORT	b. ABSTRACT	c. THIS PAGE			STI Help Desk (email:help@sti.nasa.gov)
U	U	U	UU	30	19b. TELEPHONE NUMBER *(include area code)* 301-621-0390